American Mineralogist, Volume 82, pages 870–877, 1997

Site preference of rare earth elements in fluorapatite: Binary (LREE+HREE)-substituted crystals

MICHAEL E. FLEET[1] AND YUANMING PAN[2]

[1]Department of Earth Sciences, University of Western Ontario, London, Ontario N6A 5B7, Canada
[2]Department of Geological Sciences, University of Saskatchewan, Saskatoon, Saskatchewan S7N 0W0, Canada

ABSTRACT

Crystals of binary (LREE+HREE)-bearing fluorapatite [La,Gd-FAp, Ce,Dy-FAp, Pr,Er-FAp, Eu,Lu-FAp; $Ca_{10-x-2y}Na_yREE_{x+y}(P_{1-x}Si_xO_4)_6A_2$, with x = 0.12–0.20, y = 0.26–0.42; $P6_3/m$] have been grown from H_2O-rich phosphate-fluoride melts, and their structures refined at room temperature with single-crystal X-ray intensities to R = 0.017–0.022. These binary-REE-substituted fluorapatite samples have REE site-occupancy ratios (REE-Ca2/REE-Ca1) of 2.32, and 2.32, 2.03, 1.71, respectively, which are 0.47–0.16 smaller than corresponding ratios calculated using data for reference single-REE-substituted fluorapatite. Discrepancies in intracrystalline partitioning between multiple-REE-substituted apatites and single-REE-substituted fluorapatite decrease with a decrease in REE concentration, becoming negligible at 0.2–0.3 total REE cations pfu in synthetic binary-REE-substituted fluorapatite and at trace abundances of REE in natural apatites. However, quantitative transference of laboratory REE site preferences to natural apatites is frustrated by the compositional complexity in nature. In the synthetic fluorapatite, there is a profound change in the spatial accommodation of REE in the apatite structure at about the position of Nd in the 4f transition-metal series, corresponding to the peak in the experimental uptake curve. Discrepancies in intracrystalline partitioning between binary-REE- and single-REE-substituted fluorapatite are attributed to non-ideal mixing of LREE and HREE that results in contraction of the Ca1 coordination sphere.

INTRODUCTION

Fleet and Pan (1994, 1995a) investigated the site preference of rare earth elements (REE) for the two Ca positions (Ca1 and Ca2) in the structure of apatite using X-ray structures of synthetic La-, Nd-, Gd-, and Dy-bearing fluorapatite [La-FAp, Nd-FAp, Gd-FAp, Dy-FAp; $Ca_{10-x-2y}Na_yREE_{x+y}(P_{1-x}Si_xO_4)_6F_2$, with x = 0.24–0.32, y = 0.32–0.51; $P6_3/m$]. A preliminary report of the uptake of REE by synthetic fluorapatite and a review of the crystal chemistry of REE was given in Fleet and Pan (1995b). For these synthetic single REE-substituted flourapatite samples, the REE site occupancy ratio (REE-Ca2/REE-Ca1) decreased monotonically for REE^{3+} cations through the 4f transition-metal series, from 4.04 for La-FAp to an estimated value of 0.86 for Lu-FAp (Fig. 1). It was also shown that substitution of REE for Ca leads to equalization of Ca1 and Ca2 bond valences (a correlation explored earlier by Hughes et al. 1991), and that the REE site occupancy ratio correlates directly with F bond valence.

An immediate concern of Fleet and Pan (1995a) was that their single-REE site occupancy ratios might not be quantitatively transferable to natural apatites, because REE site occupancy ratios calculated for the four natural apatites of Hughes et al. (1991) were systematically higher than the observed values (Table 1). The discrepancy between observed and calculated REE site occupancy ratios was not readily attributable to other compositional variables because the compositions of the four natural apatites of Hughes et al. (1991) encompassed the ranges in total REE cations and Na/Si cation and F/OH anion ratios investigated by Fleet and Pan (1995a). The likely temperatures of formation (or recrystallization) of the natural apatites also encompassed the crystallization temperatures of the synthetic fluorapatite samples. Thus, the discrepancy between observed and calculated REE site occupancy ratios pointed to complexity in the accommodation of REE in multiple-REE-substituted apatites.

EXPERIMENTAL PROCEDURES

Single crystals of binary-REE-substituted fluorapatite were grown from volatile-rich melts using a standard cold-seal hydrothermal reaction vessel, closely following the procedures of Fleet and Pan (1995a) for La-FAp, Gd-FAp, and Dy-FAp. Starting materials were prepared from synthetic hydroxylapatite, REE_2O_3, CaF_2, and amorphous SiO_2, and contained the equivalent of about 10 mol% $Ca_4REE_6(SiO_4)_6F_2$. Charges consisted of about 0.020 g of starting composition for each of a light REE (LREE) and heavy REE (HREE), 0.040 g of NaF, and 0.01 cm^3 of deionized water contained in a sealed gold capsule about 4 cm in length. Thus the total molar REE in the charges was the same as in Fleet and Pan (1995a)

0003–004X/97/0910–0870$05.00

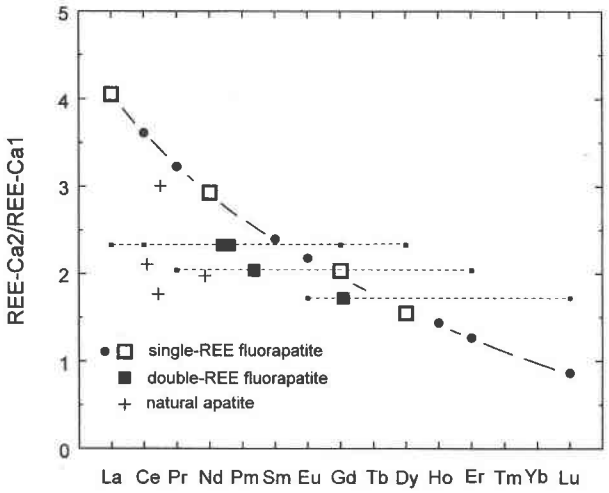

FIGURE 1. REE site-occupancy ratios determined for La-FAp,Nd-FAp,Gd-FAp, and Dy-FAp (open squares) by Fleet and Pan (1995a), with presently interpolated values for other single-REE-substituted fluorapatite samples (circles). Also shown are results for present binary-REE-substituted fluorapatite crystals (large full squares; small full squares indicate corresponding LREE-HREE pairs), and natural apatites of Hughes et al. (1991; plus signs). Average REE compositions are represented by position in the 4f transition-metal series determined from total 4f electrons per REE^{3+} cation. Trend line in this and following figures is fitted visually.

and series A experiments of Fleet and Pan (1995b). The compositions investigated in this study are La,Gd-FAp, Ce,Dy-FAp, Pr,Er-FAp, and Eu,Lu-Fap (Table 2).

The synthetic fluorapatite crystals were analyzed using a JEOL JXA-8600 Superprobe at the University of Saskatchewan (Fleet and Pan 1995a). The compositions reported in Table 3 are averages of 11 or 12 individual spot analyses.

Single-crystal measurements were made with an Enraf Nonius CAD-4F diffractometer, using graphite-monochromatized Mo$K\alpha$ X-radiation. Structure refinements followed the description given by Fleet and Pan (1995a), and experimental details are given in Table 2. The idealized formulae assumed for refinement are given in Table 3. The crystals of Ce,Dy-FAp and Eu,Lu-FAp were twinned (twin axis: [0001]). For these two crystals, the observed structure factors were corrected for the contribution from twinning after the procedure of Fleet and Burns (1990), yielding twin proportions of 0.371 and 0.416, respectively. In Fleet and Burns (1990) and this study, twin proportions were determined by iteration (cf. Sasaki et al. 1980). For simple incoherent twinning, this method is preferred over least-squares refinement, which might explore false correlations between twin proportion and crystal-structure parameters. Final parameters are given in Table 4, and observed and calculated structure factors in Table 5[1].

TABLE 1. REE site-occupancy ratios for natural apatites

Apatite	REE-Ca2/REE-Ca1 Observed*	Calculated†	Difference	Total REE (pfu)	4f electrons per REE^{3+}‡
Pajarito	1.76	3.42	−1.66	1.21	1.43
Oka-B	2.10	3.56	−1.46	0.84	1.09
Kipawa	1.97	2.86	−0.89	0.51	2.85
Oka	3.00	3.39	−0.39	0.20	1.50

* Hughes et al. (1991).
† Using site-occupancy ratios for synthetic single-REE-substituted fluorapatite (Fig. 1); see text.
‡ With Y considered as Ho.

DISCUSSION

Uptake of REE

Bond distances and bond angles for the four binary-REE-substituted fluorapatite crystals are compared in Table 6 and Figure 2. Substitution of even small amounts of REE has a significant effect on the structure of apatite (e.g., Hughes et al. 1991; Fleet and Pan 1995a). Ideally, a comparison of structural features should be made between fluorapatite samples of similar contents of individual REE or total REE and charge-balancing substituents. This is clearly impractical both for natural apatite and synthetic fluorapatite because of the variability of natural compositions and the distinctly different crystal-chemical behavior of LREE and HREE in apatite.

Fleet and Pan (1995b) reported that the uptake of REE by fluorapatite synthesized similarly to the present samples peaked at Nd. REE patterns [i.e., plots of (REE in fluorapatite)/(REE in melt)] were convex upward and LREE enriched. For their series A experiments, the REE_2O_3 content of fluorapatite crystallized with approximately 10 mol% $Ca_4REE_6(SiO_4)_6F_2$ in the starting composition varied from 9.9 wt% in Lu-FAp to 12 wt% in Nd-FAp and 3.2 wt% in Lu-FAp. Thus, although each of the present experiments had starting compositions containing approximately 10 mol% $Ca_4REE_6(SiO_4)_6F_2$, we anticipated a similar systematic variation in uptake of REE, both between pairs of LREE and HREE in individual experiments and from one experiment to another. Consistent with these expectations, the uptake of REE_2O_3 was reasonably constant for La to Gd and about half of that for the series A single-REE-substituted fluorapatite samples of Fleet and Pan (1995b) but was reduced considerably for Dy to Lu (Table 3). The range in Na content (0.26–0.42 cations pfu) was comparable to that of the single-REE-substituted fluorapatite samples of Fleet and Pan (1995a; 0.32–0.51 cations pfu) but the Si contents were somewhat lower (0.12–0.20 and 0.24–0.32 cations pfu, respectively).

Thus, variation in amount of substituents is an additional factor causing variation in structural features of the

[1] For a copy of Table 5, order Document AM-97-646 from the Business Office, Mineralogical Society of America, 1015 Eighteenth Street NW, Suite 601, Washington, DC 20036, U.S.A. Please remit $5.00 in advance. Deposit items may also be available on the American Mineralogist web site; refer to inside back cover of a current issue for web address.

TABLE 2. Experimental details

	La,Gd-FAp	Ce,Dy-FAp	Pr,Er-FAp	Eu,Lu-FAp
		Synthesis		
Experiment	AP49	AP50	AP57	AP54
Temperature (°C)	680	680	690	685
Pressure (GPa)	0.12	0.12	0.13	0.12
Time* (h)	18	18	40	40
		Crystal data		
Size ($mm^3 \times 10^3$)	1.98	1.00	3.47	1.72
Shape	prism	prism	tablet	prism
Twinned	no	yes	no	yes
a (Å)	9.3940(9)	9.3874(6)	9.3845(15)	9.3812(8)
c (Å)	6.8967(3)	6.8920(3)	6.8901(6)	6.8867(4)
Volume ($Å^3$)	527.09(12)	525.91(9)	525.51(22)	524.80(12)
No. reflections	20	20	20	20
2θ range (°)	55.5–76.2	55.5–76.3	55.6–76.3	55.6–76.3
		Intensity data		
Method	θ-2θ	θ-2θ	θ-2θ	θ-2θ
Reflections	±*hkl*	±*hkl*	±*hkl*	±*hkl*
Number	3574	3579	3523	3570
Unique	1081	1077	1075	1075
Number with ($I < 3\sigma_I$)	199	125	190	103
Refined parameters	41	41	41	41
2θ range (°)	0–80	0–80	0–80	0–80
		Absorption correction		
μ (cm^{-1})	42.9	40.7	40.9	41.4
Transmission factors†	0.56–0.66	0.58–0.76	0.54–0.62	0.47–0.70
		Final refinement		
R	0.017	0.018	0.018	0.022
R_w	0.018	0.021	0.020	0.025
s	0.927	0.897	1.077	1.214
Extinction (g,‡ $\times 10^4$)	0.524(7)	1.19(1)	0.182(4)	0.59(1)
Δρ ($e/Å^3$) (+)	0.70	0.72	0.84	0.82
(−)	0.46	0.69	0.41	0.71

* Time at final temperature.
† Determined by Gaussian integration with a 12 × 12 × 12 grid.
‡ Type-I extinction (Coppens and Hamilton 1970).

present fluorapatite crystals; it is considered to be generally of second order for bond distances and angles but more important for bond valence.

Determination of site occupancies

The substitution of REE for Ca in the present synthetic fluorapatite crystals is accommodated exclusively by compensating substitutions of Si and Na for P and Ca, respectively (Rønsbo 1989; Fleet and Pan 1995a):

$$REE^{3+} + Si^{4+} = Ca^{2+} + P^{5+};$$

$$Ca_{10-x}REE_x(P_{1-x}Si_xO_4)_6A_2 \quad (1)$$

$$REE^{3+} + Na^{1+} = 2Ca^{2+};$$

$$Ca_{10-2y}Na_yREE_y(PO_4)_6A_2 \quad (2)$$

Following Fleet and Pan (1995a), Si was assigned a partial occupancy on the P position and Na was restricted to Ca1. The site occupancy of Na was refined in Fleet and Pan (1995a), resulting in a dominant preference for Ca1. The present restriction of Na to Ca1 also facilitates comparison with Hughes et al. (1991), who assigned all Na to Ca1 in their structure refinements of natural apatites to provide a limiting case for REE ordering. The present structure refinements (Tables 2 and 4) determined a combined (LREE + HREE) occupancy, using scattering factors for neutral atomic species and f' and f'' combined for the LREE and HREE pairs from the data in Tables 2.2B and 2.3.1 of the *International Tables for X-ray Crystallography* (Ibers and Hamilton 1974) in proportion to the amounts present. In summary, only the REE site occupancy of Ca2 was refined; the other site occupancies were constrained to the crystal compositions given in Table 3 using the following algorithm:

$$(Ca\text{-}Ca2)/2 = 0.5 - (REE\text{-}Ca2)/2 \quad (3)$$

$$(REE\text{-}Ca1)/3 = \Sigma REE - (REE\text{-}Ca2)/2 \quad (4)$$

$$(Ca\text{-}Ca1)/3 = \Sigma Ca - (Ca\text{-}Ca2)/2 \quad (5)$$

$$(Na\text{-}Ca1)/3 = \Sigma Na \quad (6)$$

where, ΣREE, ΣCa, and ΣNa are total REE, Ca, and Na cations, respectively, normalized to (ΣREE + ΣCa + ΣNa) = 5/6, and Ca-Ca1, Na-Ca1, REE-Ca1, Ca-Ca2, and REE-Ca2 are the site occupancies, whose final values are given in Table 7.

We attempted to extract site occupancies for individual LREE and HREE by iterative refinement of the HREE site occupancy of Ca2. However, the resulting HREE site occupancy ratios (Table 7) were erratic. Evidently, there

TABLE 3. Compositions (wt%) and formulas of synthetic REE-bearing fluorapatite

	La,Gd-FAp	Ce,Dy-FAp	Pr,Er-FAp	Eu,Lu-FAp
P_2O_5	38.8(5)	39.1(6)	39.5(5)	39.1(9)
SiO_2	1.24(11)	0.69(3)	0.75(26)	0.78(16)
CaO	47.4(7)	47.8(6)	49.6(5)	50.3(9)
Na_2O	1.23(8)	1.12(8)	0.98(16)	0.76(5)
REE_2O_3	La 4.83(37)	Ce 5.21(39)	Pr 5.50(15)	Eu 5.88(28)
	Gd 4.98(16)	Dy 2.86(10)	Er 2.25(69)	Lu 1.03(8)
F	3.25(5)	4.01(15)	3.32(12)	3.11(32)
O≡F	1.36	1.69	1.40	1.31
Total	100.4	98.8	100.5	99.7
Chemical formulas based on 16 cations				
P	5.80	5.88	5.81	5.78
Si	0.20	0.12	0.13	0.14
Ca	8.98	9.11	9.25	9.42
Na	0.42	0.39	0.33	0.26
REE	La 0.31	Ce 0.34	Pr 0.35	Eu 0.35
	Gd 0.29	Dy 0.16	Er 0.12	Lu 0.05
F	1.81	2.25	1.83	1.72
OH*	0.19	—	0.17	0.28
O	24.08	23.87	24.01	24.02
Formulas used in X-ray structure refinement				
Ca	8.97	9.11	9.20	9.34
Na	0.42	0.39	0.33	0.26
REE	La 0.31	Ce 0.34	Pr 0.35	Eu 0.35
	Gd 0.29	Dy 0.16	Er 0.12	Lu 0.05
P	5.80	5.88	5.87	5.86
Si	0.20	0.12	0.13	0.14
O	24.00	24.00	24.00	24.00
F	2.00	2.00	2.00	2.00

* OH calculated by difference.

TABLE 4. Positional and isotropic displacement parameters (Å²)

		La,Gd-FAp	Ce,Dy-FAp	Pr,Er-FAp	Eu,Lu-FAp
Ca1	x	⅔	⅔	⅔	⅔
Ca1	y	⅓	⅓	⅓	⅓
Ca1	z	0.00040(9)	0.0007(1)	0.00067(9)	0.0007(1)
Ca1	B_{eq}	0.81(1)	0.81(2)	0.81(1)	0.80(2)
Ca2	x	0.99093(5)	0.99103(6)	0.99179(5)	0.99206(6)
Ca2	y	0.24106(5)	0.24124(6)	0.24187(5)	0.24255(6)
Ca2	z	¼	¼	¼	¼
Ca2	B_{eq}	0.703(7)	0.675(8)	0.666(7)	0.630(9)
P	x	0.36875(6)	0.36863(7)	0.36854(6)	0.36854(7)
P	y	0.39774(6)	0.39783(7)	0.39757(6)	0.39764(7)
P	z	¼	¼	¼	¼
P	B_{eq}	0.475(6)	0.480(8)	0.485(7)	0.492(9)
O1	x	0.4838(2)	0.4845(2)	0.4839(2)	0.4843(2)
O1	y	0.3256(2)	0.3257(2)	0.3258(2)	0.3258(2)
O1	z	¼	¼	¼	¼
O1	B_{eq}	0.93(2)	0.94(2)	0.93(2)	0.95(2)
O2	x	0.4667(2)	0.4665(2)	0.4670(2)	0.4665(2)
O2	y	0.5869(2)	0.5865(2)	0.5876(2)	0.5870(2)
O2	z	¼	¼	¼	¼
O2	B_{eq}	1.11(2)	1.08(2)	1.09(2)	1.17(3)
O3	x	0.2561(1)	0.2563(1)	0.2564(1)	0.2566(2)
O3	y	0.3405(1)	0.3408(2)	0.3406(1)	0.3414(2)
O3	z	0.0715(1)	0.0713(2)	0.0710(2)	0.0706(2)
O3	B_{eq}	1.31(2)	1.30(2)	1.25(2)	1.16(2)
F	x	0	0	0	0
F	y	0	0	0	0
F	z	¼	¼	¼	¼
F	B_{eq}	2.46(7)	2.32(7)	2.26(7)	2.57(9)

Note: $B_{eq} = \frac{4}{3} \Sigma_i \Sigma_j \beta_{ij} a_i \cdot a_j$.

was too little electron density contrast for meaningful refinement, e.g., for La,Gd-FAp, the maximum possible difference in electrons on Ca1 and Ca2 obtained by arbitrarily partitioning La and Gd was only 32% of one electron (i.e., equivalent to ⅓ of an H atom).

There is an important distinction between the refinement procedures of Fleet and Pan (1995a) and the present study and those of Hughes et al. (1991), which was overlooked in Fleet and Pan (1995a). Whereas only one site occupancy (that of Ca2) was refined in our studies, Hughes et al. (1991) considered their REE values to be only semiquantitative and, therefore, refined the occupancies of Ca1 and Ca2 simultaneously. This open refinement of Ca1 and Ca2 may introduce error in site occupancies because of unaccounted for atomic charges (e.g., Sasaki et al. 1980) and limitations in the experimental data. For the present synthetic fluorapatite crystals, the Hughes et al. (1991) procedure does result in a slight increase in the REE site-occupancy ratio (the values for unconstrained refinement in Table 7). Nevertheless, we feel that difference in refinement procedure does not have a significant bearing on the difference in site-occupancy ratios between Hughes et al. (1991) and our studies.

Calculated site-occupancy ratios

For a more detailed comparison between the refined site occupancies of the natural and synthetic apatites, we have calculated site-occupancy ratios for the natural REE-bearing apatites of Hughes et al. (1991) and the present fluorapatite samples using the measured and interpolated ratios for the single-REE substituted fluorapatite samples (Tables 1 and 7; Fig. 3). However, the interpolated ratios have been estimated more precisely than in Fleet and Pan (1995a), using the curvilinear distribution of the measured ratios (Fig. 1). The revised series of single-REE site occupancy ratios is: La 4.04, Ce 3.61, Pr 3.22, Nd 2.92,

TABLE 6. Selected bond distances (Å) and angles (°)

	La,Gd-FAp	Ce,Dy-FAp	Pr,Er-FAp	Eu,Lu-FAp
Ca1-O1 × 3	2.407(1)	2.400(1)	2.403(1)	2.400(1)
Ca1-O2* × 3	2.461(1)	2.461(1)	2.457(1)	2.457(1)
Ca1-O3† × 3	2.818(1)	2.813(1)	2.814(1)	2.806(2)
Mean	2.562	2.558	2.558	2.554
Ca2-O1†	2.671(1)	2.672(1)	2.675(1)	2.676(2)
Ca2-O2‡	2.383(0)	2.381(1)	2.371(1)	2.369(1)
Ca2-O3 × 2	2.504(1)	2.503(1)	2.499(1)	2.499(1)
Ca2-O3§ × 2	2.353(1)	2.351(1)	2.349(1)	2.347(1)
Mean	2.461	2.460	2.457	2.456
Ca2-F	2.308(0)	2.308(0)	2.309(1)	2.314(1)
P-O1	1.536(1)	1.541(2)	1.535(1)	1.538(2)
P-O2	1.539(1)	1.534(2)	1.544(1)	1.539(1)
P-O3 × 2	1.535(1)	1.533(1)	1.534(1)	1.534(1)
Mean	1.536	1.535	1.537	1.536
O1-P-O2	111.25(8)	111.10(10)	111.14(8)	111.17(11)
O1-P-O3‖ × 2	111.05(5)	111.07(6)	111.03(5)	111.15(7)
O2-P-O3 × 2	108.32(5)	108.27(6)	108.21(5)	107.95(7)
O3-P-O3‖	106.69(8)	106.89(9)	107.06(8)	107.29(10)

* $-x, -y, -z$.
† $-y, x - y, z$.
‡ $y - x, -x, z$.
§ $x - y, x, -z$.
‖ $x, y, ½ - z$.

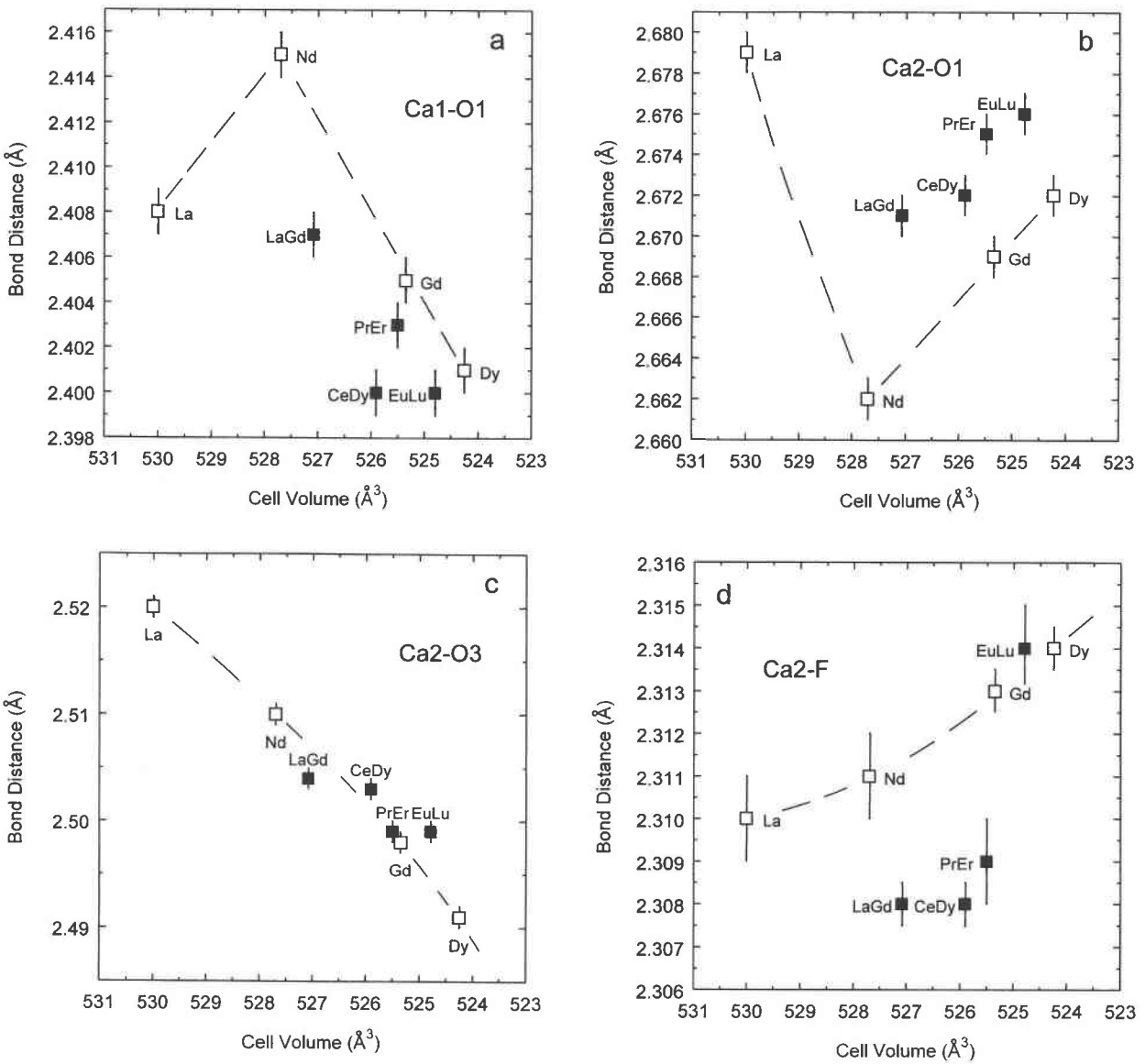

FIGURE 2. Variation in Ca1-O1 (**a**), Ca2-O1 (**b**), Ca2-O3 (**c**), and Ca2-F (**d**) bond distances in fluorapatite with REE substitution for present binary-REE compositions (full squares) and single-REE compositions of Fleet and Pan (1995a; open squares). Note that (Ca1-O1)- and (Ca2-O1)-cell volume distributions have a distinct maximum and minimum, respectively, near Nd.

Sm 2.39, Eu 2.17, Gd 2.03, Dy 1.54, Ho(Y) 1.43, Er 1.26, and Lu 0.86, with uncertainties varying from ±0.01 for La to ±0.15 for Lu.

The procedure for calculating site-occupancy ratios assumed that the contents per formula unit of individual REE in Ca1 and Ca2 positions given by the site-occupancy ratios of synthetic single-REE-substituted fluorapatite (Fig. 1) were additive in multiple-REE-substituted apatite. This assumption is clearly limited to ideal mixing on both Ca1 and Ca2 sites and dilute solution. The contents per formula unit of individual REE in Ca1 and Ca2 (REE^{Ca1}, REE^{Ca2}) were recovered from the corresponding single-REE-substituted fluorapatite site-occupancy ratio (R) using:

$$A = R/(1 + R) \quad (7)$$

$$B = (REE^{Ca1} + REE^{Ca2})/\{(A \times 6) + [(1 - A) \times 4]\} \quad (8)$$

$$REE^{Ca1} = (1 - A) \times 4 \times B \quad (9)$$

$$REE^{Ca2} = A \times 6 \times B. \quad (10)$$

Controls on REE site occupancies

We suggest below that discrepancies in the quantitative site partitioning of REE in natural and synthetic apatites (Table 1 and 7; Fig. 3) are attributable to difference in REE concentration, spatial accommodation of individual REE, and crystal-chemical behavior of LREE and HREE.

TABLE 7. REE site occupancies and site-occupancy ratios*

		La,Gd-FAp	Ce,Dy-FAp	Pr,Er-FAp	Eu,Lu-FAp
Ca1 site occupancy	Ca	0.861	0.876	0.888	0.908
	Na	0.105	0.097	0.083	0.065
	REE	0.034	0.028	0.029	0.028
Ca2 site occupancy	Ca	0.921	0.935	0.941	0.952
	REE	0.079(1)	0.065(1)	0.059(1)	0.048(1)
Ratio (constrained refinement†)		2.32	2.32	2.03	1.71
Ratio (calculated†)	LREE	4.04	3.61	3.22	2.17
	HREE	2.03	1.54	1.26	0.86
	Crystal	2.80	2.61	2.40	1.88
Δ(observed − calculated) ratio		−0.47	−0.29	−0.37	−0.16
Ratio (unconstrained refinement‡)		2.53	2.72	2.22	1.92
Ratio for HREE by iteration		13.0	1.5	10.0	0.1
Total REE (pfu)		0.606	0.504	0.474	0.404
4f electrons per REE^{3+}		3.37	3.60	4.35	7.08
Fluorine bond valence§		0.934	0.927	0.921	9.900

* REE-Ca2/REE-Ca1.
† After Fleet and Pan (1995a).
‡ Following Hughes et al. (1991).
§ After Brown (1981).

Although surface structure does indeed play an important role in the incorporation of minor and trace elements in apatite (Rakovan and Reeder 1994, 1996), there is little evidence that nonequilibrium inter- and intracrystalline partitioning is a significant factor here. The synthetic fluorapatite crystals were essentially homogeneous from core to margin. Weak oscillatory growth zoning was generally evident in backscattered-electron (BSE) images, but the actual variations in REE were fairly minimal; e.g., for series A Pr-FAp from Fleet and Pan (1995b), 12 EPMA spot analyses representing a core-to-margin cross section with the beam positioned variously on bands of bright and dark contrast yielded an average value for Pr_2O_3 of 10.2 ±0.4 wt%. Sector zoning was weakly developed in some crystals but the BSE contrast for it was appreciably less than that for the oscillatory zoning.

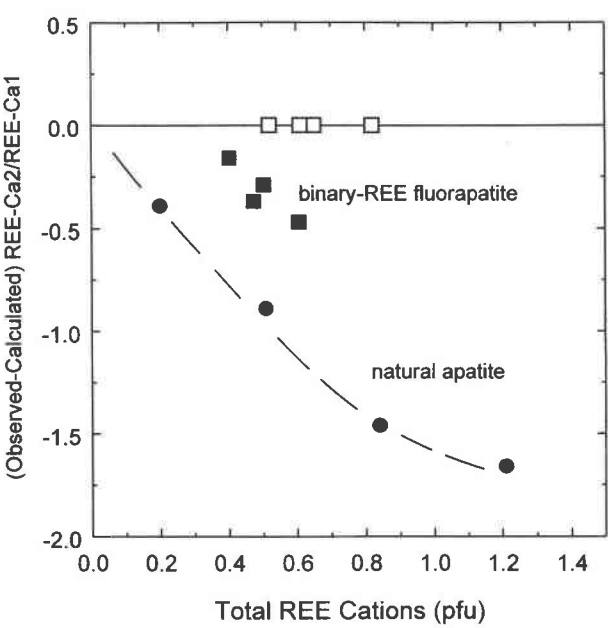

FIGURE 3. Variation of difference in observed and calculated REE site occupancy ratio of apatites with REE abundance; circles are natural apatites of Hughes et al. (1991), full squares are present binary-REE-substituted fluorapatite, and open squares are single-REE-substituted fluorapatite of Fleet and Pan (1995a).

Fleet and Pan (1995a) had noted that, of the four apatites investigated by Hughes et al. (1991), the sample with lowest REE abundance (Oka) had an REE site-occupancy ratio most consistent with the single-REE-substituted fluorapatite values. It is now apparent that discrepancies between the observed and calculated site-occupancy ratios vary systematically with total REE cations, becoming zero for trace abundances of REE (Fig. 3). The discrepancies for the present binary-REE-substituted fluorapatite crystals behave similarly and possibly would be negligible at 0.2–0.3 total REE cations pfu (Fig. 3).

We emphasize that the discrepancies between the observed and calculated site occupancies of the natural apatites (Table 1; Fig. 3) do not reflect error in the site occupancies determined in Hughes et al. (1991) or Fleet and Pan (1995a), or limitation in the method of calculation. Possible errors in assumed REE compositions and refinement procedures are relatively minor, and, as noted in Fleet and Pan (1995a), the REE compositions of the natural apatites in question are dominated by Ce.

As discussed in Fleet and Pan (1995a), the preferential substitution of LREE in natural apatite results in increase in size of the structure (Hughes et al. 1991). For a given stereochemical environment, R^{3+} of La and Ce is greater than R^{2+} of Ca, and the latter generally corresponds to R^{3+} of Nd (cf. Shannon 1976). Fleet and Pan (1995a) reported that many crystal-chemical parameters for single-REE-substituted fluorapatite (e.g., unit-cell volume, bond distances, F bond valence) generally decreased monotonically through the 4f transition-metal series. This implied that structural change in response to spatial accommodation of REE varied monotonically also. Fleet

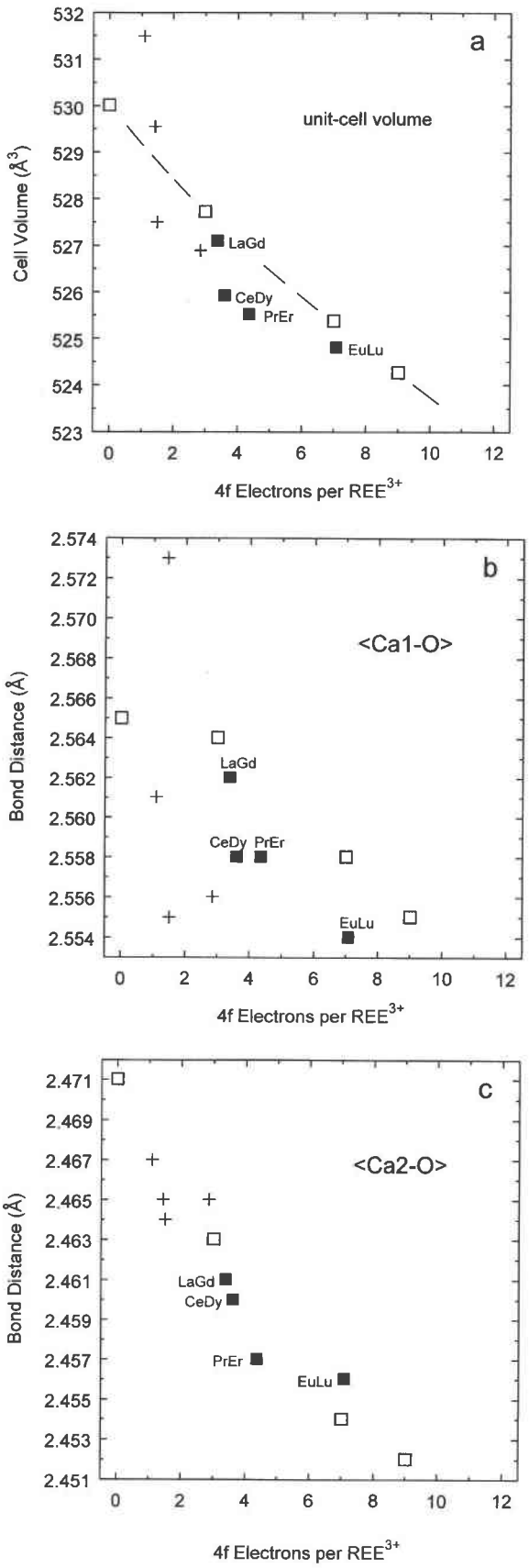

FIGURE 4. Unit-cell volume (**a**) and mean Ca1-O (**b**) and Ca2-O (**c**) bond distances for the binary-REE-substituted fluorapatite structures (full squares) compared with data for single-REE-substituted fluorapatite (open squares; Fleet and Pan 1995a) and natural apatites (plus signs; Hughes et al. 1991).

→

and Pan (1995a) did observe that some Ca-O distances varied erratically with REE substitution. Closer inspection of these structural data (Table 5[1] of Fleet and Pan 1995a) reveals that the Ca1-O1, Ca2-O1, P-O1, and P-O2 bond distances and O1-P-O2 bond angle for Nd-FAp are distinctly anomalous. In fact, the distributions of these bond distances and bond angle do not vary monotonically but are hinged at Nd (e.g., Fig. 2). The (Ca1-O1)-cell volume distribution has a distinct maximum near Nd (Fig. 2a), which corresponds to a greater than expected mean Ca1-O bond distance for Nd-FAp (Fig. 4b). Conversely, the (Ca2-O1)-cell volume distribution has a distinct minimum near Nd, but the mean Ca2-O bond distance is apparently not anomalously low compared to the trend for single-REE-substituted fluorapatite (Fig. 4c). Furthermore, the Ca1-O1 and Ca2-O1 bond distances for the binary-REE-substituted fluorapatite crystals are also consistent with a hinge in the vicinity of Nd (Figs. 2a and 2b).

Thus, there is a profound change in the accommodation of REE by the apatite structure in the vicinity of Nd, with the precise position in the 4f transition-metal series depending on the nature of other substituents. The hinge position in the 4f transition-metal series corresponds to the maximum in the uptake patterns of REE by fluorapatite (Fleet and Pan 1995b; work in progress) and is probably related to the correspondence in effective ionic radii of Ca^{2+} and Nd^{3+}. Such structural complexity is not unexpected. Although the effective ionic and crystal radii of REE do vary monotonically through the 4f transition-metal series (e.g., Fleet and Pan 1995b), the response of the apatite structure to the spatial accommodation of even ideally spherical REE^{3+} cations will not be isotropic. Even if the Ca1 and Ca2 coordination spheres could vary independently of the more strongly bonded PO_4 tetrahedra, their site symmetries are only 3 and *m*, respectively. The Jahn-Teller effect may contribute to the distortion in Ca1-O bond distances near Nd, but crystal-field contributions to the stability of REE in apatite are expected to be weak (e.g., Fleet and Pan 1995b).

Unit-cell volume and mean Ca-O distances for the binary-REE-substituted fluorapatite structures are compared with data for single-REE-substituted fluorapatite in Figure 4, with position in the 4f transition-metal series determined from total 4f electrons per REE^{3+} cation. It is evident that unit-cell volumes of the binary-REE-substituted fluorapatite structures are consistently smaller than expected from the monotonic distribution for the single-REE-substituted fluorapatite structures, and this is accounted for mainly by a decrease in mean Ca1-O dis-

tance, and Ca2-F distance (Fig. 2d). Evidently, the accommodation of individual REE in fluorapatite is not independent of other REE substituents. Non-ideal mixing effects are more evident where an LREE is mixed with an HREE, as in the present binary-REE-substituted fluorapatite crystals. The relative contraction in the Ca1 coordination sphere of the binary-REE-substituted fluorapatite structure is mainly in the Ca1-O1 bond distance (Fig. 2a). We note that the average REE compositions of the binary-REE-substituted fluorapatite samples, represented by total 4f electrons per REE^{3+} cation, lie beyond the hinge in the 4f transition-metal series (Figs. 2a and 2b) and all unit-cell volumes are reduced (Fig. 4a).

The present study stresses the influence of spatial accommodation on REE site occupancy and structural change in apatite, whereas Fleet and Pan (1995a) also placed emphasis on bond valence. Any fine control exerted by bond valence in the present structures is obscured by variation in the proportions of substituents. However, calculated bond valence remains a very powerful first-approximation technique for deducing the REE site preference of apatites and end-member calc-silicate structures (Fleet and Pan 1995a, 1995b; Pan and Fleet 1996).

A detailed crystal-chemical explanation for the lower REE site-occupancy ratios of the natural apatites of Hughes et al. (1991; present Fig. 1) is obscured by compositional complexity. With the single exception of Ca2-O1, the Ca-O bond distances of the natural apatites increase progressively with REE substitution as expected, and mean Ca2-O distances are consistent with the trend for REE-substituted synthetic fluorapatite (Fig. 4c). However, unit-cell volumes and mean Ca1-O distances vary erratically (Figs. 4a and 4b), showing a marked control by other substituents (i.e., Na, Si, and OH). As with the binary-REE-substituted fluorapatite, it is the Ca1 coordination sphere that is most sensitive to multiple substitution of the Ca positions by REE.

The consequences of a profound change caused by accommodating REE, in the vicinity of Nd, by the structure of synthetic fluorapatite for the REE geochemistry of apatite and its host rocks are uncertain. Apatite has only a weak selectivity among REE and its REE composition in a given rock type generally reflects the whole-rock abundance of these elements (e.g., Fleischer and Altschuler 1986; Fleet and Pan 1995a, 1995b; Chazot et al. 1996). However, this is because REE generally partition much more strongly into apatite than co-existing rock-forming silicates. The relative preference of LREE, and Nd in particular, for apatite is then obscured by the analytical uncertainty. Somewhat different results have been obtained for in situ analysis of apatites in some metasomatic and metamorphic rocks (Fleet and Pan 1995b), which have REE patterns that are convex upward and either peaked or have inflections near Nd.

Acknowledgments

We thank R.T. Downs and J.M. Hughes for helpful comments on the manuscript, T. Bonli for assistance with EPMA, and the Natural Sciences and Engineering Research Council of Canada for financial support.

References cited

Brown, I.D. (1981) The bond-valence method: An empirical approach to chemical structure and bonding. In M. O'Keeffe and A. Navrotsky, Eds., Structure and bonding in crystals II, p. 1–30. Academic Press, New York.

Chazot, G., Menzies, M.A., and Harte, B. (1996) Determination of partition coefficients between apatite, clinopyroxene, amphibole, and melt in natural spinel lherzolites from Yemen: Implications for wet melting of the lithospheric mantle. Geochimica et Cosmochimica Acta, 60, 423–437.

Coppens, P. and Hamilton, W.C. (1970) Anisotropic extinction correction in the Zachariasen approximation. Acta Crystallographica, A26, 71–83.

Fleet, M.E. and Burns, P.C. (1990) Structure and twinning of cobaltite. Canadian Mineralogist, 28, 719–723.

Fleet, M.E. and Pan, Y. (1994) Site preference of Nd in fluorapatite $[Ca_{10}(PO_4)_6F_2]$. Journal of Solid State Chemistry, 111, 78–81.

———(1995a) Site preference of rare earth elements in fluorapatite. American Mineralogist, 80, 329–335.

———(1995b) Crystal chemistry of rare earth elements in fluorapatite and some calc-silicates. European Journal of Mineralogy, 7, 591–605.

Fleischer, M. and Altschuler, Z.S. (1986) The lanthanides and yttrium in minerals of the apatite group-an analysis of the available data. Neues Jahrbuch für Mineralogie Monatschefte, 10, 467–480.

Hughes, J.M., Cameron, M., and Mariano, A.N. (1991) Rare-earth-element ordering and structural variations in natural rare-earth-bearing apatites. American Mineralogist, 76, 1165–1173.

Ibers, J.A. and Hamilton, W.C., Eds. (1974) International tables for X-ray crystallography, vol. IV, 366 p. Kynoch, Birmingham, U.K.

Pan, Y. and Fleet, M.E. (1996) Intrinsic and external controls on the incorporation of rare-earth elements in calc-silicate minerals. Canadian Mineralogist, 34, 147–159.

Rakovan, J. and Reeder, R.J. (1994) Differential incorporation of trace elements and dissymmetrization in apatite: The role of surface structure during growth. American Mineralogist, 79, 892–903.

———(1996) Intracrystalline rare earth element distributions in apatite: Surface structural influences on incorporation during growth. Geochimica et Cosmochimica Acta, 60, 4435–4445.

Rønsbo, J.G. (1989) Coupled substitutions involving REEs and Na and Si in apatites in alkaline rocks from the Ilimaussaq intrusion, South Greenland, and the petrological implications. American Mineralogist, 74, 896–901.

Sasaki, S., Fujino, K., Takéuchi, Y, and Sadanaga, R. (1980) On the estimation of atomic charges by the X-ray method for some oxides and silicates. Acta Crystallographica, A36, 904–915.

Shannon, R.D. (1976) Revised effective ionic radii and systematic studies of interatomic distances in halides and chalcogenides. Acta Crystallographica, A32, 751–767.

Manuscript received September 19, 1996
Manuscript accepted April 29, 1997